

# Spin exchange rates in proton-hydrogen collisions

Steven R. Furlanetto<sup>1\*</sup> & Michael R. Furlanetto<sup>2†</sup>

<sup>1</sup>*Yale Center for Astronomy and Astrophysics, Yale University, PO Box 208121, New Haven, CT 06520-8121*

<sup>2</sup>*Physics Division, Los Alamos National Laboratory, MS H803, P.O. Box 1663, Los Alamos NM 87545*

13 June 2021

## ABSTRACT

The spin temperature of neutral hydrogen, which determines the optical depth and brightness of the 21 cm line, is determined by the competition between radiative and collisional processes. Here we examine the role of proton-hydrogen collisions in setting the spin temperature. We use recent fully quantum-mechanical calculations of the relevant cross sections, which allow us to present accurate results over the entire physically relevant temperature range 1–10<sup>4</sup> K. For kinetic temperatures  $T_K \gtrsim 100$  K, the proton-hydrogen rate coefficient exceeds that for hydrogen-hydrogen collisions by about a factor of two. However, at low temperatures ( $T_K \lesssim 5$  K) H–H<sup>+</sup> collisions become several thousand times more efficient than H–H and even more important than H–e<sup>−</sup> collisions.

**Key words:** atomic processes – scattering – diffuse radiation

## 1 INTRODUCTION

The 21 cm transition is potentially a powerful probe of the pre-ionization intergalactic medium (IGM) because of the enormous amount of neutral hydrogen in the Universe at that time (Field 1958; Scott & Rees 1990; Madau et al. 1997). It can teach us about reionization, the formation of the first structures and the first galaxies, and even the “dark ages” before these objects formed (Furlanetto et al. 2006, and references therein). It is therefore crucial to understand the fundamental physics underlying the 21 cm transition. One critical aspect is the spin temperature, which is determined by the competition between the scattering of cosmic microwave background (CMB) photons, the scattering of Ly $\alpha$  photons (Wouthuysen 1952; Field 1958), and collisions. When CMB scattering dominates, the IGM remains invisible because the spin temperature approaches that of the CMB (which is used as a backlight).

Before star formation commences, collisions are the only way to break this degeneracy. The total coupling rate is determined by collisions with other hydrogen atoms, protons, and electrons. At the low residual electron fraction expected after cosmological recombination (Seager et al. 1999), H–H collisions dominate. Spin exchange in such interactions has received a great deal of attention over the years (Purcell & Field 1956; Smith 1966; Allison & Dalgarno 1969; Zygelman 2005; Hirata & Sigurdson 2006). We have also recently re-examined spin-exchange in H–e<sup>−</sup> collisions using accurate numerical cross-sections including the  $L = 0$ –3 partial waves (Furlanetto & Furlanetto 2007) and showed that such collisions become important when the ionized fraction  $x_i \gtrsim 0.01$ .

However, proton-hydrogen collisions have received little attention in the literature; Smith (1966) provided the most recent evaluation of their spin-exchange rate coefficient, but he used only semi-classical estimates of the cross sections. In the intervening years, atomic physicists have calculated the relevant quantum mechanical cross sections to high accuracy using increasingly sophisticated numerical techniques (e.g., Hunter & Kuriyan 1977; Hodges & Breig 1991; Krstić & Schultz 1999b; Krstić et al. 2004). Our purpose here will be to generate similarly accurate rate coefficients from the Krstić et al. (2004) cross sections for use in 21 cm calculations. We will show that, at sufficiently low temperatures, H–H<sup>+</sup> collisions could dominate the spin coupling, but that in more realistic circumstances they provide only a small correction to the usual calculation.

The remainder of this paper is organized as follows. In §2, we briefly review the 21 cm transition. Our main results are contained in §3, where we calculate the spin de-excitation rates for H–H<sup>+</sup> collisions. We conclude and discuss applications to the 21 cm transition in the high-redshift IGM in §4.

## 2 THE 21 CM TRANSITION

We review the relevant characteristics of the 21 cm transition here; we refer the interested reader to Furlanetto et al. (2006) for a more comprehensive discussion. The 21 cm brightness temperature (relative to the CMB) of a patch of the IGM is

$$\delta T_b = 27 x_{\text{HI}} (1 + \delta) \left( \frac{\Omega_b h^2}{0.023} \right) \left( \frac{0.15}{\Omega_m h^2} \frac{1+z}{10} \right)^{1/2} \times \left( \frac{T_S - T_\gamma}{T_S} \right) \left[ \frac{H(z)/(1+z)}{dv_{\parallel}/dr_{\parallel}} \right] \text{ mK}, \quad (1)$$

\* Email: steven.furlanetto@yale.edu

† Email: mfurlanetto@lanl.gov

where  $\delta$  is the fractional overdensity,  $x_{\text{HI}}$  is the neutral fraction,  $T_S$  is the spin temperature,  $T_\gamma$  is the CMB temperature, and  $dv_{\parallel}/dr_{\parallel}$  is the gradient of the proper velocity along the line of sight. The last factor accounts for redshift-space distortions (Bharadwaj & Ali 2004; Barkana & Loeb 2005).

The spin temperature  $T_S$  is determined by competition between scattering of CMB photons, scattering of UV photons (Wouthuysen 1952; Field 1958), and collisions (Purcell & Field 1956). In equilibrium,

$$T_S^{-1} = \frac{T_\gamma^{-1} + x_c T_K^{-1} + x_\alpha T_c^{-1}}{1 + x_c + x_\alpha}, \quad (2)$$

where  $T_K$  is the kinetic temperature of the gas,  $T_c$  is the color temperature of the radiation field at the Ly $\alpha$  transition, and the  $x_i$  are coupling coefficients. The last part of this equation describes the Wouthuysen-Field effect, in which the absorption and re-emission of Ly $\alpha$  photons mixes the hyperfine states (Wouthuysen 1952; Field 1958). We refer the reader to Furlanetto et al. (2006), and references therein, for more detail on this component.

The factor  $x_c$  is the total collisional coupling coefficient, including H–H, H–e $^-$ , and H–H $^+$  collisions. In this paper, we will focus only on the contribution from proton-hydrogen collisions, which we will denote  $x_c^{\text{pH}}$ ; the other components are  $x_c^{\text{HH}}$  and  $x_c^{\text{eH}}$ , with obvious meanings (see Zygelman 2005 and Furlanetto & Furlanetto 2007 for the most recent estimates). In more detail,

$$x_c^{\text{pH}} = \frac{n_p \kappa_{10}^{\text{pH}} T_\star}{A_{10} T_\gamma}, \quad (3)$$

where  $\kappa_{10}^{\text{pH}}$  is the spin de-excitation rate in proton-hydrogen collisions,  $n_p$  is the local proton density,  $T_\star \equiv h\nu_{21}/k_B = 0.068$  K,  $\nu_{21}$  is the frequency of the 21 cm line, and  $A_{10} = 2.85 \times 10^{-15} \text{ s}^{-1}$  is the Einstein- $A$  coefficient for that transition.

### 3 PROTON-HYDROGEN COLLISIONS

#### 3.1 The spin exchange cross section

We must first compute the cross section for spin exchange as a function of collision energy. To do so, we begin by noting that the radial wave functions in the H–H $^+$  system satisfy the Schrödinger equations in uncoupled partial waves of angular momentum  $L$ . In the energy range with which we are concerned, these become

$$\left[ \frac{d^2}{dR^2} - \frac{L(L+1)}{R^2} - 2\mu E_i(R) + 2\mu E \right] \Psi_i^{(L)}(R) = 0, \quad (4)$$

where  $R$  is the internuclear distance,  $\mu$  is the reduced mass,  $E_i$  is the adiabatic electronic potential for the  $1s\sigma_g$  (gerade) or  $2p\sigma_u$  (ungerade) states of H $_2^+$ , and  $\Psi_i$  is the radial wave function for the appropriate channel.

We assume the process to be electronically elastic, so that the scattering problem can be reduced in the usual way to the computation of phase shifts  $\delta_L^g$  and  $\delta_L^u$  (see Furlanetto & Furlanetto 2007 for a description of the analogous transformation for H–e $^-$  scattering). The so-called charge transfer cross section  $\sigma_{\text{ct}}$  may then be written (e.g., Krstić et al. 2004)

$$\sigma_{\text{ct}} = \frac{4\pi}{k^2} \sum_{L=0}^{\infty} (2L+1) \sin^2(\delta_L^g - \delta_L^u), \quad (5)$$

where  $k$  is the center-of-mass momentum. This cross section is defined with reference to an experiment in which a beam of polarized

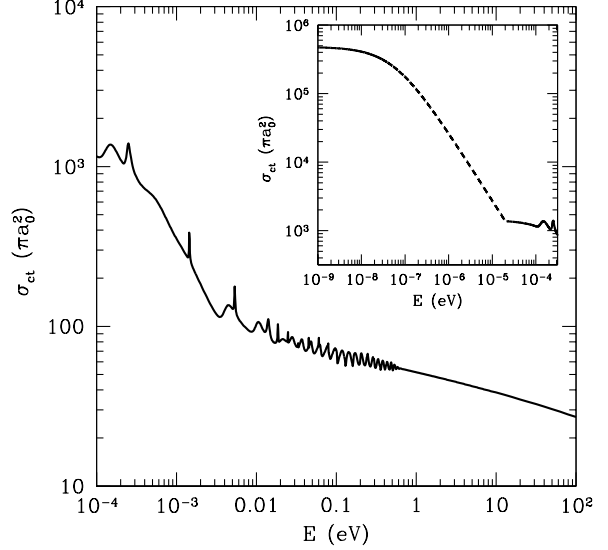


**Figure 1.** Charge transfer cross section (in units of  $\pi a_0^2$ ) for H–H $^+$  collisions, as a function of the collision energy. The solid curve shows  $\sigma_{\text{ct}}$  from Krstić et al. (2004). The dashed curve in the inset shows the effective range approximation for the low energy behavior (see text).

protons (with, say, spin +1/2) is incident on an unpolarized collection of hydrogen atoms and in which the spins of the scattered protons are measured, so that protons with spin –1/2 can be unambiguously determined to have originated in the target. It tends to the usual charge transfer cross section in the classically distinguishable particle limit (Krstić & Schultz 1999a).

This cross section must be calculated numerically, and there is a long history of such attempts (Hunter & Kuriyan 1977; Hodges & Breig 1991; Krstić & Schultz 1999b). For  $10^{-4} \text{ eV} < E < 10^2 \text{ eV}$ , we use the most recent calculations, from Krstić et al. 2004, which are accurate numerically to six significant figures, although the neglect of coupling to higher electronic states reduces the accuracy somewhat at the upper end of the energy range.

Figure 1 shows the resulting cross section, in units of  $\pi a_0^2$  (where  $a_0$  is the Bohr radius) over this entire energy range. Note the rich structure in  $\sigma_{\text{ct}}$ , especially at moderately small energies. This is in sharp contrast to the H–e $^-$  cross section, which is smooth until the neighborhood of the  $n = 2$  excitation threshold (see Fig. 1 in Furlanetto & Furlanetto 2007). Capturing this detailed structure required the use of a closely-spaced energy grid (664 points were used here) and the inclusion of high- $L$  partial waves (up to  $L_{\text{max}} = 3200$  at 100 eV; Krstić et al. 2004). The narrow features are caused by shape resonances in the electronic potentials and have the usual Fano line shape. The broader features, known as “Regge oscillations,” have a more subtle origin. They are generated by combinations of one to three poles in the  $S$ -matrix, each of which corresponds to one of the  $L = 0$  vibrational bound states of H $_2^+$ . These features are difficult to understand in the traditional partial wave representation, but their nature has recently been explained using the Mulholland representation (Macek et al. 2004). Note that the charge transfer cross section shows significantly less structure than the elastic cross section, which also includes broad oscillations at higher energies due to the glory effect (Child 1984).

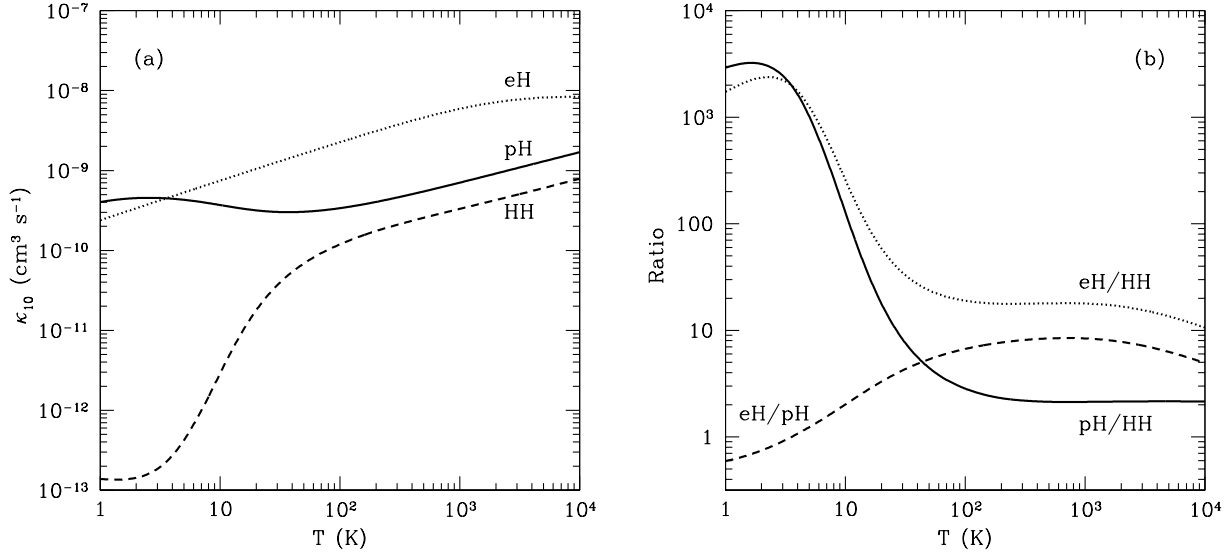


**Figure 2.** Spin-exchange rate coefficients. (a): Rate coefficients for H–H<sup>+</sup> collisions (solid curve), H–e<sup>+</sup> collisions (dotted curve, from Furlanetto & Furlanetto 2007), and H–H collisions (dashed curve, from Zygelman (2005)). (b): Ratios between the three rate coefficients in panel a.

These calculations ignored non-adiabatic and relativistic effects, so they were not extended below  $\sim 10^{-4}$  eV, where such phenomena become significant. Instead, we use the numerically converged low-energy cross sections of Glassgold et al. (2005). These calculations used the same technique as Krstić et al. (2004), and thus also neglected non-adiabatic and relativistic effects, but they at least provide us with a baseline estimate of the collision behavior at small energies. They show that only the  $L = 0$  terms remain non-zero at low energies, and  $\delta_0^g \rightarrow n\pi$  as  $E \rightarrow 0$ . In this limit,

$$\sigma_{ct} \approx \frac{4\pi}{k^2} \sin^2 \delta_0^u, \quad (6)$$

which is one-quarter of the total elastic cross section. Meanwhile, effective-range theory yields an excellent approximation for  $\delta_0^u$ :

$$k \cot \delta_0^u = -\frac{1}{a} + \frac{\pi\alpha}{3a^2}k + \frac{2\alpha}{3a}k^2 \ln\left(\frac{\alpha k^2}{16}\right) + O(k^3), \quad (7)$$

where the scattering length  $a = 801.2 a_0$  and the polarizability  $\alpha = 4.5 a_0^3$  parameterize the polarization potential of the hydrogen atom (Glassgold et al. 2005).

The resulting cross section is shown for  $10^{-10}$  eV  $< E < 10^{-4}$  eV by the inset in Figure 1. We use the effective-range approximation for  $E < 2 \times 10^{-5}$  eV and linearly interpolate the cross section between that value and  $10^{-4}$  eV (where Glassgold et al. 2005 showed that the effective range approximation for the total cross section breaks down). This effective range theory approximation provides a good match to numerical calculations of the spin-exchange cross section (using methods similar to Glassgold et al. 2005) in this energy regime (P. Krstić, private communication). Although we do not know how strongly the relativistic and non-adiabatic corrections will affect the cross sections, we do not expect them to have a dramatic effects on our final results, as discussed below.

### 3.2 The spin-exchange rate coefficient

To apply this to H–H<sup>+</sup> collisions in the IGM, we must thermally average the above cross sections. The spin-exchange rate coefficient relevant for our purposes is

$$\kappa_{10}^{\text{pH}} = \sqrt{\frac{8k_B T_K}{\pi\mu}} \left( \frac{3}{16} \sigma_{ct} \right), \quad (8)$$

where  $k_B$  is Boltzmann’s constant,  $T_K$  is the kinetic temperature of the IGM, and the prefactor with the square root is the thermally-averaged velocity. The factor 3/16 appears because the cross section as defined above assumes a polarized beam of electrons, while here we care about the net rate at which spin de-excitation occurs (Smith 1966; Krstić & Schultz 1999a). We must therefore multiply  $\sigma_{ct}$  by 1/4 (the probability that the target atom has  $F = 0$ ) and then 3/4 (the probability that the scattered atom has  $F = 1$ ).

The solid line in Figure 2a shows  $\kappa_{10}^{\text{pH}}$  over the full temperature range of interest. It is much smoother than  $\sigma_{ct}$ , because the thermal averaging washes out the resonances. At moderate to high temperatures, the rate coefficient is roughly proportional to  $T_K^{1/2}$ , because  $\sigma_{ct}$  is itself falling only slowly with energy. However, at lower temperatures the cross section increases rapidly, so that  $\kappa_{10}^{\text{pH}}$  is actually the largest rate coefficient at  $T_K \lesssim 3$  K. This is in sharp contrast to hydrogen-hydrogen and hydrogen-electron collisions, whose rate coefficients are shown by the dashed and dotted lines, respectively. The H–e<sup>+</sup> cross section increases as  $E \rightarrow 0$ , but only modestly (see Fig. 1 of Furlanetto & Furlanetto 2007), while the H–H rate decreases rapidly as  $E \rightarrow 0$  (see below).

Figure 2b compares these three processes in more detail, showing the ratios between the various cross sections. At extremely small temperatures, H–H<sup>+</sup> collisions can be the dominant process. Electron-hydrogen collisions quickly come to dominate at  $T_K \gtrsim 3$  K, and remain more important at all higher temperatures. Naively, we would expect that  $\kappa_{10}^{\text{eH}}/\kappa_{10}^{\text{pH}} \sim \sqrt{m_H/2m_e} \sim 30$ . In reality, the ratio is several times smaller than that, because

**Table 1.** Proton-hydrogen spin de-excitation rate coefficients

$T_K$ (K)	$\kappa_{10}^{\text{pH}} (10^{-9} \text{ cm}^3 \text{ s}^{-1})$	$T_K$ (K)	$\kappa_{10}^{\text{pH}} (10^{-9} \text{ cm}^3 \text{ s}^{-1})$
1	0.4028	1000	0.7051
2	0.4517	2000	0.9167
5	0.4301	3000	1.070
10	0.3699	5000	1.301
20	0.3172	7000	1.480
50	0.3047	10,000	1.695
100	0.3379	15,000	1.975
200	0.4043	20,000	2.201
500	0.5471		

proton-hydrogen collisions have a substantially larger cross section throughout this temperature range.<sup>1</sup>

Figure 2b also shows that, at high temperatures, H–H<sup>+</sup> collisions are marginally more efficient than H–H collisions (by about a factor of two); the shapes of these two rate coefficients mirror each other quite closely in this regime. However, at lower temperatures, proton-hydrogen collisions are vastly more efficient. As we have seen, the  $L = 0$  term in  $\sigma_{\text{ct}}$  approaches a large constant value; in the analogous H–H problem, the corresponding quantity actually approaches zero because of an accidental cancellation in the  $S$ -wave cross sections (Zygelman 2005; Sigurdson & Furlanetto 2006)

For use in other calculations, we present in Table 1 our results for  $\kappa_{10}^{\text{pH}}$  as a function of temperature. These are fully numerically converged to the six significant figure accuracy of the Krstić et al. (2004) cross sections, but as emphasized above they do not include all the relevant physical processes across the entire temperature range. In particular, at the lower end of the temperature range, non-adiabatic processes and relativistic corrections lead to uncertainties at the per cent level. For example, assuming that the cross section is constant below  $10^{-4}$  eV changes our final results by (5, 1, 0.2) per cent at  $T_K = (1, 3.7, 10)$  K, respectively. At the upper end of the temperature range, rotational coupling of the  $2p\sigma_u$  and  $2p\pi_u$  states affects the rate coefficients at the  $\sim 0.1$  per cent level.

## 4 DISCUSSION

We have computed the rate coefficients for spin-exchange in H–H<sup>+</sup> collisions using recent, fully quantum mechanical solutions for the relevant cross sections over most of the energy range of interest (Krstić et al. 2004). We have also extended the calculation to lower temperatures ( $T_K \sim 1$  K) by using the approximate cross sections of Glassgold et al. (2005); while these ignore non-adiabatic effects and relativistic corrections, they appear to be accurate to several per cent.

Our results (collected in numerical form in Table 1) will be particularly useful for calculating the spin temperature of the high-redshift IGM before reionization (and hence brightness in the 21 cm line). Before the first luminous sources appear, this is determined purely by the competition between collisions and CMB scat-

tering. In most cases, protons contribute a small but non-negligible fraction of the coupling. For example, the standard recombination calculation yields a global ionized fraction  $x_i \sim 2 \times 10^{-4}$  and  $T_K \sim 9[(1+z)/20]^{1.85}$  K for redshifts  $z \sim 10$ –100 (Seager et al. 1999); the exponent is slightly smaller than two (which would be expected for an adiabatically-cooling non-relativistic gas) because of a small amount of Compton heating off the CMB. At the higher redshifts, where  $T_K \sim 100$  K, protons account for only  $\sim 0.04$  per cent of the total coupling, but if the gas does remain cool to  $z \sim 20$  they provide  $\sim 2$  per cent as much coupling as hydrogen-hydrogen collisions. In the unlikely event that the gas cools to  $T = 2.5$  K at  $z = 10$  without interference from luminous sources, we would have  $x_e^{\text{pH}}/x_c^{\text{HH}} \sim 0.6$  – and protons would become even more important than electrons.

In reality, the first galaxies probably appear at  $z \gtrsim 20$ . They flood the Universe with Ly $\alpha$  photons (which affect the spin temperature through the Wouthuysen-Field mechanism) and X-ray photons (which heat the gas). As a result, the spin temperature probably increases well before  $z = 10$  (Sethi 2005; Furlanetto 2006; Pritchard & Furlanetto 2006), so that protons never actually come to dominate the coupling. However, they still must be included for high-accuracy predictions of the 21 cm signal.

In this paper, we have only examined spin-exchange via electronically elastic proton-hydrogen collisions. At high temperatures, such collisions can instead excite higher atomic levels or even ionize the atom. Such processes could also affect the spin temperature because the hydrogen atom could enter a different spin state after the radiative cascade that follows. Although we do not know the relevant excitation cross sections, our experience with electron-hydrogen collisions suggests that in practice these collisions will not be important. For H–e<sup>−</sup>, the most likely transition at relatively low temperatures is excitation to the  $2p$  state, which is followed almost immediately by radiative de-excitation and emission of a Ly $\alpha$  photon. This Ly $\alpha$  photon scatters  $\sim 10^5$  times before redshifting out of resonance, so in terms of spin coupling it is much more important than the single collision that generated it. For a Maxwell-Boltzmann energy distribution, excitation of this process through electron-hydrogen collisions suddenly comes to dominate at  $T_K \sim 6300$  K (Furlanetto & Furlanetto 2007). If proton-hydrogen collisions cause similar excitations, they too would become relatively unimportant once electronic excitations become energetically feasible. Furthermore, because the electron-hydrogen rate coefficient exceeds the proton-hydrogen rate coefficient by a factor of several in this temperature range, we expect proton collisions to be only a minor perturbation. At higher temperatures, the collisionally-generated Ly $\alpha$  photons completely dominate, and the effect of  $\kappa_{10}^{\text{pH}}$  will be even smaller.<sup>2</sup>

We thank P. Krstić for making his H–H<sup>+</sup> cross section data available to us in an electronic form. This publication has been approved for release as LA-UR-07-0513. Los Alamos National Laboratory, an affirmative action/equal opportunity employer, is operated by Los Alamos National Security, LLC, for the National Nuclear Security Administration of the U.S. under contract DE-AC52-06NA25396.

<sup>1</sup> Note that the decline in  $\kappa_{10}^{\text{eH}}/\kappa_{10}^{\text{pH}}$  at  $T \gtrsim 3000$  K is somewhat artificial. Furlanetto & Furlanetto (2007) excluded all electrons with  $E > 10.2$  eV from the thermal average, because these electrons have a substantial probability of exciting the atom to higher electronic states.

<sup>2</sup> In reality, X-ray heating of the IGM results in an excess of fast electrons even when the temperature is much smaller. Thus the Ly $\alpha$  channel can be important throughout the “reheating” era (Chen & Miralda-Escude 2006; Chuzhoy et al. 2006; Pritchard & Furlanetto 2006).

## REFERENCES

- Allison A. C., Dalgarno A., 1969, *ApJ*, 158, 423  
Barkana R., Loeb A., 2005, *ApJ*, 624, L65  
Bharadwaj S., Ali S. S., 2004, *MNRAS*, 352, 142  
Chen X., Miralda-Escude J., 2006, submitted to *ApJ* (astro-ph/0605439)  
Child M. S., 1984, *Molecular Collision Theory* (Dover Publications, Inc.: Mineola, NY)  
Chuzhoy L., Alvarez M. A., Shapiro P. R., 2006, *ApJ*, 648, L1  
Field G. B., 1958, *Proc. I.R.E.*, 46, 240  
Furlanetto S. R., 2006, *MNRAS*, 371, 867  
Furlanetto S. R., Furlanetto M. R., 200, *MNRAS*, 374, 547  
Furlanetto S. R., Oh S. P., Briggs F. H., 2006, *Physics Reports*, 433, 181  
Glassgold A. E., Krstić P. S., Schultz D. R., 2005, *ApJ*, 621, 808  
Hirata C. M., Sigurdson K., 2006, submitted to *MNRAS* (astro-ph/0605071)  
Hodges Jr. R. R., Breig E. L., 1991, *J. Geophys. Research*, 96, 7697  
Hunter G., Kuriyan M., 1977, *Royal Society of London Proceedings Series A*, 353, 575  
Krstić P. S., Macek J. H., Ovchinnikov S. Y., Schultz D. R., 2004, *PRA*, 70, 042711  
Krstić P. S., Schultz D. R., 1999a, *PRA*, 60, 2118  
Krstić P. S., Schultz D. R., 1999b, *Journal of Physics B Atomic Molecular Physics*, 32, 3485  
Macek J. H., Krstić P. S., Ovchinnikov S. Y., 2004, *Physical Review Letters*, 93, 183203  
Madau P., Meiksin A., Rees M. J., 1997, *ApJ*, 475, 429  
Pritchard J. R., Furlanetto S. R., 2006, submitted to *MNRAS* (astro-ph/0607234)  
Purcell E. M., Field G. B., 1956, *ApJ*, 124, 542  
Scott D., Rees M. J., 1990, *MNRAS*, 247, 510  
Seager S., Sasselov D. D., Scott D., 1999, *ApJ*, 523, L1  
Sethi S. K., 2005, *MNRAS*, 363, 818  
Sigurdson K., Furlanetto S. R., 2006, *Physical Review Letters*, 97, 091301  
Smith F. J., 1966, *Plan. Space Sci.*, 14, 929  
Wouthuysen S. A., 1952, *AJ*, 57, 31  
Zygelman B., 2005, *ApJ*, 622, 1356